HHS Public Access

Author manuscript

J Inorg Biochem. Author manuscript; available in PMC 2018 June 01.

Published in final edited form as:

J Inorg Biochem. 2018 June ; 183: 107–116. doi:10.1016/j.jinorgbio.2018.03.007.

Interactions of iron-bound frataxin with ISCU and ferredoxin on the cysteine desulfurase complex leading to Fe-S cluster assembly

Kai Cai, **Ronnie O. Frederick**, **Marco Tonelli**, **John L. Markley***

National Magnetic Resonance Facility at Madison and Biochemistry Department, University of Wisconsin-Madison, 433 Babcock Drive, Madison, WI 53706, United States

Abstract

Frataxin (FXN) is involved in mitochondrial iron-sulfur (Fe-S) cluster biogenesis and serves to accelerate Fe-S cluster formation. FXN deficiency is associated with Friedreich ataxia, a neurodegenerative disease. We have used a combination of isothermal titration calorimetry and multinuclear NMR spectroscopy to investigate interactions among the components of the biological machine that carries out the assembly of iron-sulfur clusters in human mitochondria. Our results show that FXN tightly binds a single Fe^{2+} but not Fe^{3+}. While FXN (with or without bound Fe^{2+}) does not bind the scaffold protein ISCU directly, the two proteins interact mutually when each is bound to the cysteine desulfurase complex ($[NFS1]_2$:$[ISD11]_2$:$[Acp]_2$), abbreviated as $(NIA)_2$, where "N" represents the cysteine desulfurase (NFS1), "I" represents the accessory protein (ISD11), and "A" represents acyl carrier protein (Acp). FXN binds $(NIA)_2$ weakly in the absence of ISCU but more strongly in its presence. Fe^{2+}-FXN binds to the $(NIA)_2$-$ISCU_2$ complex without release of iron. However, upon the addition of both L-cysteine and a reductant (either reduced FDX2 or DTT), Fe^{2+} is released from FXN as consistent with Fe^{2+}-FXN being the proximal source of iron for Fe-S cluster assembly.

Keywords

Iron-binding; Iron-release; Iron-sulfur cluster assembly; Isothermal titration calorimetry; NMR spectroscopy; Protein-protein interactions

Iron-sulfur (Fe-S) clusters are ubiquitous protein cofactors that are involved in a variety of cellular processes, including respiration, electron transfer, DNA replication and repair, cofactor biosynthesis, and gene regulation [1–4]. The canonical mechanism for Fe-S cluster biogenesis involves the pyridoxal phosphate dependent enzyme cysteine desulfurase, L-

*Corresponding author at: Biochemistry Department, University of Wisconsin-Madison, 433 Babcock Drive, Madison, WI 53706, United States. jmarkley@wisc.edu (J.L. Markley).

Author contributions

K.C. and J.L.M. designed research; K.C., R.O.F. and M.T. performed research; R.O.F, M.T., and K.C. contributed new reagents/analytic tools; K.C., M.T. and J.L.M. analyzed data; and K.C. and J.L.M. wrote the paper.

Competing interests

The authors have no competing interests.

cysteine as the source of sulfur, an iron delivery protein, a reductant (ferredoxin), and a scaffold protein [5,6]. We have shown that the human scaffold protein ISCU (like its *Escherichia coli* counterpart IscU [7]) populates two interconverting conformational states: one that is structured (S), and one that is dynamically disordered (D) [8]. Human cysteine desulfurase (NFS1) differs from that of *E. coli* (IscS) by the requirement for two accessory proteins: ISD11 and mitochondrial acyl carrier protein (ACP). ISD11 (also known as LYRM4), which is a member of the 'LYRM' (Leu-Tyr-Arg motif) family of mitochondrial proteins [9], is essential both for Fe-S cluster assembly and the maintenance of cellular iron homeostasis [10]. Mitochondrial ACP is an acidic protein well known for its role in mitochondrial fatty acid synthesis (FASII) [11], but its separate role as an essential component of the human cysteine desulfurase complex that catalyzes Fe-S cluster biosynthesis has only recently come to light [12]. The desulfurase complex produced by co-expressing human ISD11 and NFS1 in *E. coli* cells contains the covalently-bound 4′-phosphopantetheine form of *E. coli* acyl carrier protein (Acp) [13]. Because this chimeric complex has been found to exhibit cysteine desulfurase activity and to support Fe-S cluster assembly *in vitro* [14], *E. coli* Acp appears to substitute for the human mitochondrial ACP. We determined the stoichiometry of the cysteine desulfurase complex as $[NFS1]_2$:$[ISD11]_2$:$[Acp]_2$ [13], hence-forth abbreviated as "$(NIA)_2$". The presence of *E. coli* Acp and this stoichiometry has been confirmed by recent X-ray structures of $(NIA)_2$ complexes produced by co-expressing human ISD11 and NFS1 in *E. coli* cells [15,16].

Ferredoxin serves as an electron donor for Fe-S cluster biosynthesis [17–20]. It has been shown that *E. coli* ferredoxin (Fdx) and the bacterial homolog of frataxin (CyaY) compete for a binding site on the *E. coli* cysteine desulfurase (IscS) [17,18]. By contrast, in eukaryotes, ferredoxin forms a larger complex with cysteine desulfurase and frataxin [19]. Human mitochondria contain two ferredoxins (FDX1 and FDX2), whose roles in Fe-S cluster assembly have been subject to debate [19,21,22]. It was shown recently that both FDX1 and FDX2 can interact with $(NIA)_2$ and donate electrons for Fe-S cluster assembly *in vitro*, although FDX2 binds more tightly and promotes more rapid cluster assembly than FDX1 [14].

The full function of human cysteine desulfurase also requires frataxin (FXN) [23,24]; defects in FXN are associated with the neurodegenerative disease Friedreich ataxia [25]. The homolog of FXN in the *E. coli* system, CyaY, paradoxically, is an inhibitor for Fe-S cluster assembly [26]; whether frataxin stimulates or inhibits depends on the nature of the cysteine desulfurase rather than on differences between human and bacterial frataxin [27,28].

We provided evidence that IscX (coded by the *isc* operon) is the iron donor in *E. coli* Fe-S cluster synthesis [29]. IscX has no eukaryotic homolog, and while FXN is a candidate, the iron donor in mitochondrial cluster assembly has not been identified definitively. There are different schools of thought regarding FXN. All agree that frataxin binds iron [30–35]. One camp holds that FXN is the iron donor [34,36–39]. Another camp contends that FXN is simply an allosteric effector [23,27,40,41].

Here, by using a combination of isothermal calorimetry (ITC), NMR spectroscopy, and *in vitro* Fe-S cluster assembly, we have delved into the molecular details of how FXN, ISCU,

and ferredoxin interact when bound to the cysteine desulfurase complex. Our results indicate that FXN-Fe^{2+} binds to the cysteine desulfurase complex when ISCU is present and only releases iron when two factors required for Fe-S cluster assembly are present (L-cysteine and reductant). These findings are consistent with Fe^{2+} bound to FXN being the proximal source of iron for Fe-S cluster assembly.

1. Results

1.1. ISCU modulates the interaction between FXN and the cysteine desulfurase complex

We prepared the cysteine desulfurase complex $(NIA)_2$ by co-expressing genes coding for NFS1 and ISD11 in *E. coli* cells. As noted above, upon purification, this yields a complex containing the holo-form of *E. coli* acyl carrier protein [13]. We used ITC to quantify the interaction of $(NIA)_2$ with ISCU and FXN (here indicating its mature form, $FXN^{81–210}$). Titration of $(NIA)_2$ with ISCU resulted in an endothermic reaction that was fitted to a 1:1 binding model with K_d = 1.7 ± 0.4 μM (Fig. 1A). Titration of $(NIA)_2$ with FXN resulted in an exothermic binding reaction that was fitted to a 1:1 binding mode with K_d = 26.2 ± 2.4 μM (Fig. 1B). The weak interaction between FXN and $(NIA)_2$ explains our inability to isolate the $(NIA)_2$-FXN_2 complex by size exclusion chromatography (SEC). Interestingly, titration of the $[NFS1]_2$:$[ISD11]_2$:$[Acp]_2$:$[ISCU]_2$ $(NIAU)_2$ complex with FXN resulted in an exothermic reaction that was fitted to a 1:1 binding mode with K_d = 3.0 ± 0.6 μM (Fig. 1C). The tighter interaction between FXN and $(NIAU)_2$ is consistent with the observation that the $[NFS1]_2$:$[ISD11]_2$: $[Acp]_2$:$[ISCU]_2$:$[FXN]_2$ $(NIAUF)_2$ complex can be readily isolated through SEC [13], as was found in several earlier studies, although the authors did not note the presence of Acp in the complex [23,41–43]. These results suggest that ISCU modulates and enhances the interaction between FXN and $(NIA)_2$.

Control ITC experiments revealed that the heats of dilution of $(NIA)_2$, FXN and ISCU were negligible (Fig. 2).

1.2. The same protein face of frataxin binds iron and the cysteine desulfurase complex

We employed nuclear magnetic resonance (NMR) spectroscopy to investigate the interaction between FXN and the cysteine desulfurase complex $(NIA)_2$. Peaks in the 2D $^{1}H,^{15}N$ TROSY-HSQC spectrum (where TROSY stands for transverse relaxation optimized spectroscopy and HSQC stands for heteronuclear single-quantum correlation) of [U-^{15}N]-FXN were identified according to assignments deposited in the Bio-MagResBank (BMRB) [44] from prior studies [45,46].

The addition of 1.0 subunit equivalent of unlabeled $(NIA)_2$ led to severe line broadening of these signals (Fig. 3A–B) as consistent with formation of a high molecular weight complex, and the subsequent addition of 1.0 subunit equivalent of unlabeled ISCU caused further peak disappearances as expected for formation of an even larger complex (Fig. 3C). Titration of a sub-stoichiometric amount (0.5 subunit equivalent) of unlabeled $(NIA)_2$ into [U-^{15}N]-FXN allowed us to map the $(NIA)_2$ binding site on FXN: the backbone $^{1}H^{N}$–$^{15}N^{H}$ peaks that were significantly shifted or broadened included those from FXN residues D104–S105,

E108–T119, D124–F127, K171–N172, and A204. Most of these residues are located on helix α1 and strand β1 of FXN (Fig. 3D and E).

1.3. Frataxin binds Fe^{2+} but not Fe^{3+}

We used NMR to investigate iron binding to FXN. The anaerobic addition of 2.0 molar equivalents of ferrous iron (Fe^{2+}) led to significant changes to the TROSY-HSQC spectrum of [U-^{15}N]-FXN (Fig. 3F–H). The peaks exhibiting chemical shift perturbations corresponded to residues D104–S105, A107–K116 and Y121–F127, most of which lie on helix α1 and strand β1 of FXN (Fig. 3I and J). These results are consistent with previous findings from iron binding to yeast [33] and human frataxin [48]. Notably, the iron-binding domain of FXN is the same as the region that is involved in the interaction with $(NIA)_2$ (Fig. 3E and J).

Previous studies suggested that FXN binds ferric iron (Fe^{3+}) as well as ferrous iron (Fe^{2+}) [36,48]; however, in our hands, the addition of a 5-fold excess of $FeCl_3$ did not lead to significant chemical shift perturbations in the TROSY-HSQC spectrum of [U-^{15}N]-FXN (Fig. 3I, green dots and Fig. 4A–C). Because we saw no evidence for precipitation of iron, the lack of an effect appears not to have been due to the low solubility of Fe^{3+} in the buffer used. To confirm this result, we carried out an experiment in which we mixed [U-^{15}N]-FXN with 2-fold ferrous iron (Fe^{2+}), and then allowed the Fe^{2+} to be oxidized by exposing the mix to O_2. Significant spectral changes resulted from the addition of Fe^{2+} (Fig. 4D). However, after Fe^{2+} oxidation, the spectrum became equivalent to that of iron-free FXN (Fig. 4E), indicating that oxidized Fe^{2+} lost affinity to FXN. Our finding of no interaction between FXN and Fe^{3+} is consistent with conclusions from a study that used X-ray absorption spectroscopy (XAS) together with extended X-ray absorption fine structure (EXAFS) [33].

1.4. FXN and ISCU do not interact on their own but interact when both are bound to $(NIA)_2$

We used a similar NMR titration approach to identify the residues of FXN that interact with the $(NIAU)_2$ complex. Titration of 0.5 subunit equivalent of unlabeled $(NIAU)_2$ into [U-^{15}N]-FXN allowed us to map the $(NIAU)_2$ binding site on FXN. In addition to the set of $^{1}H^{N}$,$^{15}N^{H}$ peaks affected by interaction with $(NIA)_2$ (Fig. 3D), another set of peaks exhibited significant shifts or line broadening in the complex containing ISCU. These peaks correspond to FXN residues I145–T149, N151–S158, K164, R165, and W168, most of which map to strands β3–β5 of FXN (Fig. 5A and B). These results suggest that the α1-β1 site of FXN forms the binding interface with $(NIA)_2$ and that strands β3–β5 of FXN are involved in the interaction with ISCU in the $(NIAU)_2$ complex. A conserved tryptophan of FXN (W155), which has been shown to be important for ISCU interaction [49], is located in strand β4 (Fig. 5B; W155 represented in stick format).

However, in the absence of $(NIA)_2$, we were unable to detect by NMR a direct interaction between FXN and ISCU, without (Fig. 6A–C) or with the presence of Fe^{2+} (Fig. 6D–F). In the presence of Fe^{2+}, we observed transfer of Fe^{2+} from FXN to ISCU, but no evidence of interaction between FXN and ISCU (Fig. 6D–F). Thus, we conclude that $(NIA)_2$ provides an anchor for each protein that leads to the observed FXN-ISCU interaction.

1.5. Iron release from FXN bound to the $(NIAU)_2$ complex requires both cysteine and reductant

A recent study suggested that FXN controls both the sulfur production and the iron entry into the $(NIAU)_2$ complex [42]. To address this issue, we investigated the iron-binding properties of FXN in the context of the cluster assembly machinery.

Several $^1H,^{15}N$ TROSY-HSQC peaks of [U-^{15}N]-FXN corresponding to FXN residues in the region of the Fe^{2+} binding site were monitored before and after adding $(NIAU)_2$. As expected, they broadened upon formation of the $(NIAU)_2$-[U-^{15}N]-FXN_2 complex (Fig. 7, row 1 and 2).

We next prepared Fe^{2+}-loaded FXN by anaerobically incubating 0.3 mM of [U-^{15}N]-FXN with 10-fold excess Fe^{2+} for 2 h and removing the excess Fe^{2+} by passage through a desalting column. We quantified the Fe^{2+} bound to FXN after desalting by using a colorimetric assay [50], and determined the Fe^{2+} content to be 0.92 ± 0.15 mol Fe^{2+}/mol FXN. Comparison of the $^1H,^{15}N$ TROSY-HSQC spectrum of [U-^{15}N]-FXN, without and with bound Fe^{2+}, revealed that iron binding led to shifts of peaks from residues D112, L113, and D115 and the disappearance of peaks from residues V125, S126, and F127 (Fig. 7A, rows 1 and 3). All these residues are located on the α1-β1 site of FXN (Fig. 7B, residues in stick representation). Then a sub-stoichiometric amount (0.5 subunit equivalent) of $(NIAU)_2$ was added to the sample of [U-^{15}N]-FXN containing Fe^{2+} and the mix was incubated for 2 h. The addition of $(NIAU)_2$ led to additional shifts in the peaks from D112, L113, and D115 and the continued disappearance of the peaks from V125, S126, and F127 (Fig. 7A, row 4). However, when a 5.0 subunit equivalent each of L-cysteine and DTT were added and the mix was incubated for 2 h, the peaks from D112, L113, and D115 shifted back toward their positions in the spectrum of iron-free FXN, and, more remarkably, the peaks from V125, S126, and F127 reappeared (Fig. 8A, row 5).

As a control, we investigated whether iron would be released with the addition of L-cysteine alone, DTT alone as the reductant, or reduced ferredoxin 2 (red-FDX2) alone as the reductant. As shown in Fig. 8, the continued broadening of ^1H-^{15}N signals under all three conditions (Fig. 8, row 4–6) indicated no iron release over a period of hours. When both L-cysteine (5.0 subunit equivalent) and red-FDX2 (2.0 subunit equivalent) were added and mix was incubated for 2 h, the peaks from V125, S126, and F127 reappeared, indicating that Fe^{2+} had been released (Fig. 9, row 7).

We interpret these results as indicating that the FXN-Fe^{2+} complex binds to the $(NIAU)_2$ complex without iron release because the iron-binding site (α1-β1) on FXN is shielded from solvent by interaction with the cysteine desulfurase complex $(NIA)_2$, but that initiation of cluster assembly by addition of L-cysteine and reductant leads to a conformational change that allows dissociation of Fe^{2+} from FXN.

1.6. Iron delivered by frataxin supports in vitro cluster assembly

Previous studies of iron-sulfur cluster assembly have utilized soluble free iron(II). We carried out a cluster assembly reaction with reduced FDX2 as the reductant and FXN loaded with Fe^{2+} as the sole iron donor to determine whether this would suffice for *in vitro* cluster

assembly. The results (Fig. 9) demonstrated that iron from Fe^{2+}-FXN and electrons provided by red-FDX2 support cluster assembly.

2. Discussion

FXN is a conserved small acidic protein that is highly expressed in tissues rich in mitochondria, such as heart, liver, and neurons [51,52]. Deficiency of FXN is associated with the neurodegenerative disease Friedreich ataxia, commonly resulting from a GAA trinucleotide repeat expansion in the *FXN* gene [25,52]. It has been shown that FXN binds iron and interacts with the core complex of Fe-S cluster biosynthesis; however, only a few molecular details of its interactions have been established.

We have shown here that FXN binds Fe^{2+} (Fig. 3) but not Fe^{3+} (Fig. 4). Neither the Fe^{2+}-bound nor the iron-free form of FXN binds to ISCU in the absence of the $(NIA)_2$ complex (Fig. 6). FXN interacts weakly with $(NIA)_2$, but the presence of ISCU greatly enhances the interaction (Fig. 1). These results are consistent with the fact that it is relatively easy to isolate the $(NIAUF)_2$ complex, as shown by previous reports [23,24,42,43]. Both the iron-free and Fe^{2+}-bound forms of FXN bind to $(NIAU)_2$.

Chemical shift perturbations of [U-^{15}N]-FXN upon titration with $(NIAU)_2$ revealed that the β3–β5 sheet region of FXN interacts with ISCU (Fig. 5). Although previous studies reported direct interactions between ISCU and FXN mediated by Fe^{2+} in the absence of $(NIA)_2$ [48,53,54], our NMR results failed to replicate such an interaction (Fig. 6). An iron-mediated interaction would be hard to understand, because the iron-binding and ISCU-binding sites on FXN are non-overlapping. We conclude that $(NIA)_2$ serves as an anchor that allows FXN and ISCU to physically interact. This view is reinforced by recent findings on *E. coli* and yeast proteins [55,56]. Mutations of residues in the β3–β5 sheet of FXN, including I154F and W155R, are linked to certain forms of Friedreich ataxia [57]. Several lines of evidence have established that the conserved W155 on the β-sheet of FXN is involved in the interaction with ISCU [43,49,55,57], and our results are consistent with these findings. Interestingly, the conserved '^{99}LPPVK^{103}' motif of ISCU, which interacts with HSP70 [58], also interacts with FXN as shown by a recent study in yeast [55].

Our NMR CS perturbation studies revealed that the highly conserved α1-β1 site of FXN participates in the binding of both Fe^{2+} and $(NIA)_2$ (Fig. 3). The α1-β1 site constitutes an acidic ridge that has been shown previously to bind Fe^{2+} and to be essential for the function of FXN [33,48]; mutation of residues on this acidic ridge have been shown to severely impair the Fe-S cluster metabolism in yeast [59]. Shielding of the iron-binding site on FXN by its interaction with the cysteine desulfurase complex $(NIA)_2$ may explain why Fe^{2+} is blocked from transfer to ISCU in the $(NIAU)_2$ complex (Figs. 7 and 8). Apparently, this shielding remains in the presence of added L-cysteine or reductant alone (Fig. 8). However, the addition of both L-cysteine and reductant (DTT or reduced FDX2) leads to the release of iron (Figs. 7 and 8). These two factors (L-cysteine and reductant) are required to activate the cysteine desulfurase which converts L-cysteine to L-alanine with the generation of sulfur. Presumably, activation of the cysteine desulfurase leads to a conformational change that allows iron release. Although the present results do not prove that the released iron is picked

up by ISCU and used for Fe-S cluster formation, we have shown that Fe^{2+}-FXN can serve as the sole iron donor for this process *in vitro* (Fig. 9). Further studies are needed to determine the nature of the conformational changes of the core complex that leads to iron release and the steps involved in transferring sulfur and iron to ISCU for Fe-S cluster assembly. Although our data show iron-bound FXN can serve as the iron donor *in vitro*, they do not rule out the existence of other iron sources *in vivo*.

Our results demonstrate that desulfurase activation by L-cysteine, electron transfer from ferredoxin, and iron entry are closely coupled, as suggested by a previous study [42]. The discovery of a frataxin-bypassing Isu1 mutant in yeast presented a strong argument against the role of FXN as the primary iron source for mitochondrial Fe-S cluster biogenesis [60–63]. A plausible scenario is that FXN receives a single Fe^{2+} from a primary iron source, binds to the cysteine desulfurase-ISCU complex and positions the Fe^{2+} in an optimal position for transfer to ISCU, but holds onto the Fe^{2+} until the cysteine desulfurase has been activated by the presence of L-cysteine and the donation of an electron from ferredoxin. FXN has been shown to directly enhance the sulfur transfer from NFS1 to ISCU [40,41].

Our current model of the mechanism of mitochondrial Fe-S cluster assembly consists of the following steps. It starts with the recruitment of ISCU by $(NIA)_2$ to form $(NIAU)_2$. Then, reduced ferredoxin (X) and Fe^{2+}-FXN (F) bind to yield $(NIAUFX)_2$. Binding of FXN opens up the active site of NFS1 allowing the entry of L-cysteine, which upon conversion to L-alanine generates S^0 bound to the active site cysteine (C381) of NFS1. An electron from reduced ferredoxin converts the bound sulfur to a radical anion (–S•), which is transferred to one of the cysteine residues of ISCU (the identity of that residue remains in question [41,64–66]). Then an electron transferred from Fe^{2+} to the radical anion leads to the formation of $–S^{2–}$ and Fe^{3+}. In the next stage, FXN and oxidized ferredoxin are released. Ferredoxin is reduced by ferredoxin reductase (FDXR), which binds to the same surface of ferredoxin that binds NFS1 [14,67], and Fe^{2+}-FXN is regenerated with Fe^{2+} from a yet to be identified mitochondrial iron protein. Then reduced ferredoxin and Fe^{2+}-FXN bind back to the $(NIAU)_2$ complex, and the cycle is repeated to complete the assembly of a [2Fe-2S] cluster. Further studies are needed to verify this mechanism and to determine if Fe^{2+} is released from FXN prior to electron transfer or if its conversion to Fe^{3+} is the cause of its release.

3. Materials and methods

3.1. Protein expression and purification

Samples of unlabeled ISCU, $(NIA)_2$, FDX2 and unlabeled and [U-^{15}N]-$FXN^{81–210}$ were produced and purified as described previously [8,13,14].

3.2. NMR Spectroscopy

NMR spectra were collected at the National Magnetic Resonance Facility at Madison on 600 or 750 MHz (^{1}H) Bruker NMR spectrometers equipped with *z*-gradient cryogenic probes. The buffer used for NMR samples (HNT buffer) contained 20 mM HEPES at pH 7.6, 150 mM NaCl, 2 mM TCEP, and 8% D_2O as the lock signal. Chemical shifts

are relative to internal DSS. All samples were filtered through a 0.22 μm centrifuge tube filter (Sigma-Aldrich) before being transferred into NMR tubes. All sample temperatures were regulated at 25 °C. NMRPipe software was used to process the raw NMR data [68] and NMRFAM-SPARKY [69] software was utilized to visualize and analyze the processed NMR data.

To study the interactions of FXN with $(NIA)_2$ and $(NIAU)_2$, 0.3 mM samples of [U-^{15}N]-FXN in HNT buffer were placed in 5 mm Shigemi NMR tubes, and 2D ^{1}H,^{15}N TROSY-HSQC spectra were collected before and after titration of these samples with unlabeled $(NIA)_2$ or $(NIAU)_2$. To study binding of Fe^{2+} to FXN, samples of 0.3 mM [U-^{15}N]-FXN were prepared in an anaerobic chamber (Coy Laboratory) without and with added $Fe_2(NH_4)_2(SO_4)_2$ and transferred to Wilmad NMR tubes equipped with air-tight seals in the anaerobic chamber. Fe^{2+} solutions were prepared anaerobically by dissolving $Fe_2(NH_4)_2(SO_4)_2$ inside the anaerobic chamber. To study binding to Fe^{3+}, $FeCl_3$ was added to 0.3 mM [U-^{15}N]-FXN; alternatively a sample of the [U-^{15}N]-FXN-Fe^{2+} complex prepared as described above in the anaerobic chamber was exposed to air and allowed to oxidize. To study the effect of Fe^{2+} bound to FXN, 2-fold of Fe^{2+} was added anaerobically to 0.2 mM [U-^{15}N]-FXN, and a 2D ^{1}H,^{15}N TROSY-HSQC spectrum was taken. Then Fe^{2+} was oxidized by exposing the solution to air and bubbling O_2 gas into the solution over a two-hour period, and a 2D ^{1}H,^{15}N TROSY-HSQC was retaken.

Chemical shift perturbations ($\Delta\delta_{HN}$ absolute value ppm) were calculated by Eq. (1):

$$\Delta\delta_{HN} = [(\Delta\delta_H)^2 + (\Delta\delta_N/6)^2]^{1/2} \quad (1)$$

where $\Delta\delta_H$ and $\Delta\delta_N$ are the chemical shift changes in the ^{1}H and ^{15}N dimensions, respectively.

The NMR peak lists relevant to Figs. 3–6 have been deposited at the BMRB under accession number 27171.

3.3. Isothermal titration calorimetry (ITC) measurement

A Nano ITC system (TA Instruments) was used to investigate interactions of $(NIA)_2$, FXN and ISCU. Proteins were dialyzed overnight in the HNT buffer. The experiments were conducted at 25 °C. For the heat of dilution control experiment of $(NIA)_2$, the syringe (volume 50 μL) contained 1.1 mM $(NIA)_2$ and the sample cell (169 μL) contained HNT buffer. For the heat of dilution control experiments of ISCU and FXN, the syringe (volume 50 μL) contained HNT buffer and the sample cell (169 μL) contained 0.1 mM ISCU or FXN. For the ITC experiment between FXN and $(NIA)_2$, the syringe contained 0.8 mM $(NIA)_2$ and the sample cell (169 μL) contained 0.07 mM FXN. For the ITC experiment between FXN and $(NIAU)_2$, the syringe contained 0.7 mM $(NIAU)_2$ and the sample cell (169 μL) contained 0.05 mM FXN. For the ITC experiment between ISCU and $(NIA)_2$, the syringe contained 1.1 mM $(NIA)_2$ and the sample cell (169 μL) contained 0.1 mM ISCU. For all the experiments, 20 2.5 μL aliquots of the sample in the syringe were injected into the solution in the sample cell, and the heat generated was measured. The ITC data processing and fitting were conducted using NanoAnalyse Software (TA Instruments).

3.4. In vitro Fe-S cluster assembly reaction

The *in vitro* Fe-S cluster reconstitution assay was carried out as follows. The reaction mixture (1 mL) prepared in the anaerobic chamber contained 100 μM red-FDX2 as the reductant, 5 μM $(NIA)_2$, 50 μM ISCU, and 100 μM Fe^{2+}-FXN. Fe^{2+}-FXN was prepared by anaerobically incubating FXN with 10-fold excess Fe^{2+} for 2 h and removing the excess Fe^{2+} by passage through a Zeba Spin desalting column (Thermo Fisher). All the protein samples were buffer-exchanged extensively prior to the experiment with anaerobic buffer containing 20 mM HEPES at pH 7.6, 150 mM NaCl (HN buffer). L-cysteine (final concentration 250 μM) was added to initiate the experiment, and the sample was then transferred to 1-cm path-length quartz cuvette, sealed with rubber septa; uv/vis spectra were collected with 5-min intervals on a Shimadzu UV-1700 spectrophotometer at 25 °C. The oxidation of reduced ferredoxin is proportional to Fe-S cluster assembly on ISCU (the electrons provided by ferredoxins are utilized for Fe-S cluster formation). Despite the spectral overlap of the signals from oxidized FDX2 and the Fe-S cluster, the increase at 456 nm can be used as a means to assess the cluster assembly rates. This was earlier verified by separating [2Fe-2S]-ISCU from oxidized FDX2 prior to collecting the spectrum at 456 nm [14].

3.5. Quantification of iron binding to FXN after desalting

Fe^{2+} was quantified by a colorimetric assay as described previously [50]. 200 μL of 12 M HCl was added to 20 μL of 0.26 mM Fe^{2+}-FXN after desalting. The concentration of FXN was determined from absorbance at 280 nm with an assumed extinction coefficient of 30,940 M^{-1} cm^{-1}. The mixture was heated to 95 °C for 15 min. The precipitate was removed by centrifugation at 14000 rpm for 5 min. The supernatant was then transferred to a 1.5 mL Eppendorf tube and diluted to 1 mL with water, and the pH of the solution was adjusted to 6.0. 5 μL of 0.15 M 1,10-phenanthroline (Phen, Sigma-Aldrich) in DMSO was added to the solution, leading to formation of the red Fe^{2+}-Phen complex. All the above procedures were done inside the anaerobic chamber to avoid oxidation of Fe^{2+}. After incubating for 30 min, the solution was transferred to a 1-cm path-length quartz cuvette, sealed with a rubber septum, and the absorbance at 510 nm was recorded on a Shimadzu UV-1700 spectrophotometer. The experiment was performed in triplicate, and the concentration of Fe^{2+} was determined by comparison to a standard curve obtained from known concentration of Fe^{2+}.

Acknowledgments

This work was initiated with support from NIH Grants U01GM094622 (which funded the Partnership for High-Throughput Enabled Biology of the Mitochondrial Proteome) and P41 GM103399 (which funds the National Magnetic Resonance Facility at Madison). Recent funding has been from the Department of Biochemistry, University of Wisconsin-Madison.

Abbreviations

Acp
holo-form of *E. coli* acyl carrier protein

ACP

holo-form of mature human mitochondrial acyl carrier protein;

BMRB
BioMagResBank

CS
chemical shift

CyaY
frataxin (*E. coli*)

DTT
dithiothreitol

E. coli
Escherichia coli

Fe-S
iron-sulfur

Fdx
ferredoxin (*E. coli*)

FDX2
ferredoxin 2 (human mitochondrial)

FXN
the mature from of human frataxin ($FXN^{81–210}$)

HSP70
molecular chaperone belonging to the heat shock protein 70 family (human mitochondrial)

HSQC
heteronuclear single-quantum correlation

ISC
iron sulfur cluster

IscS
cysteine desulfurase (*E. coli*)

IscU
scaffold protein for Fe-S cluster assembly (*E. coli*)

ISCU
scaffold protein for Fe-S cluster assembly (human mitochondrial)

IscX
iron-binding protein (*E. coli*)

ISD11
(also known as LYRM4) small protein that binds tightly to NFS1 and is required for its activity

ITC
isothermal titration calorimetry

$(NIA)_2$
$[NFS1]_2$:$[ISD11]_2$:$[Acp]_2$

$(NIAU)_2$
$[NFS1]_2$:$[ISD11]_2$:$[Acp]_2$:$[ISCU]_2$

$(NIAUF)_2$
$[NFS1]_2$:$[ISD11]_2$:$[Acp]_2$:$[ISCU]_2$:$[FXN]_2$

NFS1
cysteine desulfurase (human mitochondrial)

NMR
nuclear magnetic resonance

PDB
Protein Data Bank

red-FDX2
reduced FDX2

SEC
size exclusion chromatography

TROSY
transverse relaxation optimized spectroscopy

[U-^{15}N]
uniform labeling with the stable isotope nitrogen-15

Phen
1,10-phenanthroline

LYRM
Leu-Tyr-Arg Motif

XAS
X-ray absorption spectroscopy

EXAFS
extended X-ray absorption fine structure

References

1. Johnson DC, Dean DR, Smith AD, Johnson MK. Annu Rev Biochem. 74 2005; :247–281. [PubMed: 15952888]
2. Fontecave M. Nat Chem Biol. 2 2006; :171–174. [PubMed: 16547473]
3. Rouault TA. Nat Rev Mol Cell Biol. 16 2015; :45–55. [PubMed: 25425402]
4. Lill R. Nature. 460 2009; :831–838. [PubMed: 19675643]
5. Py B, Barras F. Nat Rev Microbiol. 8 2010; :436–446. [PubMed: 20467446]
6. Lill R, Muhlenhoff U. Annu Rev Cell Dev Biol. 22 2006; :457–486. [PubMed: 16824008]
7. Kim JH, Tonelli M, Markley JL. Proc Natl Acad Sci U S A. 109 2012; :454–459. [PubMed: 22203963]
8. Cai K, Frederick RO, Kim JH, Reinen NM, Tonelli M, Markley JL. J Biol Chem. 288 2013; :28755–28770. [PubMed: 23940031]
9. Angerer H. Biochem Soc Trans. 41 2013; :1335–1341. [PubMed: 24059529]
10. Shi Y, Ghosh MC, Tong WH, Rouault TA. Hum Mol Genet. 18 2009; :3014–3025. [PubMed: 19454487]
11. Kastaniotis AJ, Autio KJ, Keratar JM, Monteuuis G, Makela AM, Nair RR, Pietikainen LP, Shvetsova A, Chen Z, Hiltunen JK. Biochim Biophys Acta. 1862 2017; :39–48.
12. Van Vranken JG, Jeong MY, Wei P, Chen YC, Gygi SP, Winge DR, Rutter J. elife. 5 2016;
13. Cai K, Frederick RO, Tonelli M, Markley JL. ACS Chem Biol. 12 2017; :918–921. [PubMed: 28233492]
14. Cai K, Tonelli M, Frederick RO, Markley JL. Biochemistry. 56 2017; :487–499. [PubMed: 28001042]
15. Cory SA, Van Vranken JG, Brignole EJ, Patra S, Winge DR, Drennan CL, Rutter J, Barondeau DP. Proc Natl Acad Sci U S A. 114 2017; :E5325–E5334. [PubMed: 28634302]
16. Boniecki MT, Freibert SA, Muhlenhoff U, Lill R, Cygler M. Nat Commun. 8 2017; :1287. [PubMed: 29097656]
17. Kim JH, Frederick RO, Reinen NM, Troupis AT, Markley JL. J Am Chem Soc. 135 2013; :8117–8120. [PubMed: 23682711]
18. Yan R, Konarev PV, Iannuzzi C, Adinolff S, Roche B, Kelly G, Simon L, Martin SR, Py B, Barras F, Svergun DI, Pastore A. J Biol Chem. 288 2013; :24777–24787. [PubMed: 23839945]
19. Webert H, Freibert SA, Gallo A, Heidenreich T, Linne U, Amlacher S, Hurt E, Muhlenhoff U, Banci L, Lill R. Nat Commun. 5 2014; :5013. [PubMed: 25358379]
20. Yan R, Adinolff S, Pastore A. Biochim Biophys Acta. 1854 2015; :1113–1117. [PubMed: 25688831]
21. Shi Y, Ghosh M, Kovtunovych G, Crooks DR, Rouault TA. Biochim Biophys Acta. 1823 2012; :484–492. [PubMed: 22101253]
22. Sheftel AD, Stehling O, Pierik AJ, Elsasser HP, Muhlenhoff U, Webert H, Hobler A, Hannemann F, Bernhardt R, Lill R. Proc Natl Acad Sci U S A. 107 2010; :11775–11780. [PubMed: 20547883]
23. Tsai CL, Barondeau DP. Biochemistry. 49 2010; :9132–9139. [PubMed: 20873749]
24. Fox NG, Das D, Chakrabarti M, Lindahl PA, Barondeau DP. Biochemistry. 54 2015; :3880–3889. [PubMed: 26016518]
25. Vaubel RA, Isaya G. Mol Cell Neurosci. 55 2013; :50–61. [PubMed: 22917739]
26. Adinolff S, Iannuzzi C, Prischi F, Pastore C, Iametti S, Martin SR, Bonomi F, Pastore A. Nat Struct Mol Biol. 16 2009; :390–396. [PubMed: 19305405]
27. Bridwell-Rabb J, Iannuzzi C, Pastore A, Barondeau DP. Biochemistry. 51 2012; :2506–2514. [PubMed: 22352884]
28. Cai K, Tonelli M, Frederick RO, Markley JL. Biochemistry. 57 2018; :1491–1500. [PubMed: 29406711]
29. Kim JH, Bothe JR, Frederick RO, Holder JC, Markley JL. J Am Chem Soc. 136 2014; :7933–7942. [PubMed: 24810328]

30. Cavadini P, O'Neill HA, Benada O, Isaya G. Hum Mol Genet. 11 2002; :217–227. [PubMed: 11823441]
31. He YN, Alam SL, Proteasa SV, Zhang Y, Lesuisse E, Dancis A, Stemmler TL. Biochemistry. 43 2004; :16254–16262. [PubMed: 15610019]
32. Bencze KZ, Kondapalli KC, Cook JD, McMahon S, Millan-Pacheco C, Pastor N, Stemmler TL. Crit Rev Biochem Mol Biol. 41 2006; :269–291. [PubMed: 16911956]
33. Cook JD, Bencze KZ, Jankovic AD, Crater AK, Busch CN, Bradley PB, Stemmler AJ, Spaller MR, Stemmler TL. Biochemistry. 45 2006; :7767–7777. [PubMed: 16784228]
34. Kondapalli KC, Kok NM, Dancis A, Stemmler TL. Biochemistry. 47 2008; :6917–6927. [PubMed: 18540637]
35. Correia AR, Wang T, Craig EA, Gomes CM. Biochem J. 426 2010; :197–203. [PubMed: 20001966]
36. Yoon T, Cowan JA. J Am Chem Soc. 125 2003; :6078–6084. [PubMed: 12785837]
37. Gerber J, Muhlenhoff U, Lill R. EMBO Rep. 4 2003; :906–911. [PubMed: 12947415]
38. Isaya G, O'Neill HA, Gakh O, Park S, Mantcheva R, Mooney SM. Acta Paediatr. (Suppl 93) 2004; :68–71.
39. Li H, Gakh O, Smith DYT, Isaya G. J Biol Chem. 284 2009; :21971–21980. [PubMed: 19491103]
40. Bridwell-Rabb J, Fox NG, Tsai CL, Winn AM, Barondeau DP. Biochemistry. 53 2014; :4904–4913. [PubMed: 24971490]
41. Parent A, Elduque X, Cornu D, Belot L, Le Caer JP, Grandas A, Toledano MB, D'Autreaux B. Nat Commun. 6 2015; :5686. [PubMed: 25597503]
42. Colin F, Martelli A, Clemancey M, Latour JM, Gambarelli S, Zeppieri L, Birck C, Page A, Puccio H, Ollagnier de Choudens S. J Am Chem Soc. 135 2013; :733–740. [PubMed: 23265191]
43. Schmucker S, Martelli A, Colin F, Page A, Wattenhofer-Donze M, Reutenauer L, Puccio H. PLoS One. 6 2011; :e16199. [PubMed: 21298097]
44. Ulrich EL, Akutsu H, Doreleijers JF, Harano Y, Ioannidis YE, Lin J, Livny M, Mading S, Maziuk D, Miller Z, Nakatani E, Schulte CF, Tolmie DE, Kent Wenger R, Yao H, Markley JL. Nucleic Acids Res. 36 2008; :D402–408. [PubMed: 17984079]
45. Kondapalli KC, Bencze KZ, Dizin E, Cowan JA, Stemmler TL. Biomol NMR Assign. 4 2010; :61–64. [PubMed: 20108066]
46. Musco G, Stier G, Kolmerer B, Adinolff S, Martin S, Frenkiel T, Gibson T, Pastore A. Structure. 8 2000; :695–707. [PubMed: 10903947]
47. Dhe-Paganon S, Shigeta R, Chi YI, Ristow M, Shoelson SE. J Biol Chem. 275 2000; :30753–30756. [PubMed: 10900192]
48. Huang J, Dizin E, Cowan JA. J Biol Inorg Chem. 13 2008; :825–836. [PubMed: 18425540]
49. Leidgens S, De Smet S, Foury F. Hum Mol Genet. 19 2010; :276–286. [PubMed: 19884169]
50. Agustina E, Goak J, Lee S, Seo Y, Park JY, Lee N. Chemistryopen. 4 2015; :613–619. [PubMed: 26491641]
51. Anzovino A, Lane DJ, Huang ML, Richardson DR. Br J Pharmacol. 171 2014; :2174–2190. [PubMed: 24138602]
52. Campuzano V, Montermini L, Molto MD, Pianese L, Cossee M, Cavalcanti F, Monros E, Rodius F, Duclos F, Monticelli A, Zara F, Canizares J, Koutnikova H, Bidichandani SI, Gellera C, Brice A, Trouillas P, De Michele G, Filla A, De Frutos R, Palau F, Patel PI, Di Donato S, Mandel JL, Cocozza S, Koenig M, Pandolfo M. Science. 271 1996; :1423–1427. [PubMed: 8596916]
53. Cook JD, Kondapalli KC, Rawat S, Childs WC, Murugesan Y, Dancis A, Stemmler TL. Biochemistry. 49 2010; :8756–8765. [PubMed: 20815377]
54. Wang T, Craig EA. J Biol Chem. 283 2008; :12674–12679. [PubMed: 18319250]
55. Manicki M, Majewska J, Ciesielski S, Schilke B, Blenska A, Kominek J, Marszalek J, Craig EA, Dutkiewicz R. J Biol Chem. 289 2014; :30268–30278. [PubMed: 25228696]
56. Prischi F, Konarev PV, Iannuzzi C, Pastore C, Adinolff S, Martin SR, Svergun DI, Pastore A. Nat Commun. 1 2010; :95. [PubMed: 20981023]

57. Li H, Gakh O, Smith DYt, Ranatunga WK, Isaya G. J Biol Chem. 288 2013; :4116–4127. [PubMed: 23269675]
58. Hoff KG, Cupp-Vickery JR, Vickery LE. J Biol Chem. 278 2003; :37582–37589. [PubMed: 12871959]
59. Foury F, Pastore A, Trincal M. EMBO Rep. 8 2007; :194–199. [PubMed: 17186026]
60. Yoon H, Knight SAB, Pandey A, Pain J, Turkarslan S, Pain D, Dancis A. PLoS Genet. 11 2015;
61. Yoon H, Knight SA, Pandey A, Pain J, Zhang Y, Pain D, Dancis A. Biochem J. 459 2014; :71–81. [PubMed: 24433162]
62. Yoon H, Golla R, Lesuisse E, Pain J, Donald JE, Lyver ER, Pain D, Dancis A. Biochem J. 441 2012; :473–480. [PubMed: 21936771]
63. Pandey A, Gordon DM, Pain J, Stemmler TL, Dancis A, Pain D. J Biol Chem. 288 2013; :36773–36786. [PubMed: 24217246]
64. Kato S, Mihara H, Kurihara T, Takahashi Y, Tokumoto U, Yoshimura T, Esaki N. Proc Natl Acad Sci U S A. 99 2002; :5948–5952. [PubMed: 11972033]
65. Smith AD, Frazzon J, Dean DR, Johnson MK. FEBS Lett. 579 2005; :5236–5240. [PubMed: 16165131]
66. Shi R, Proteau A, Villarroya M, Moukadiri I, Zhang L, Trempe JF, Matte A, Armengod ME, Cygler M. PLoS Biol. 8 2010; :e1000354. [PubMed: 20404999]
67. Kurisu G, Kusunoki M, Katoh E, Yamazaki T, Teshima K, Onda Y, Kimata-Ariga Y, Hase T. Nat Struct Biol. 8 2001; :117–121. [PubMed: 11175898]
68. Delaglio F, Grzesiek S, Vuister GW, Zhu G, Pfeifer J, Bax A. J Biomol NMR. 6 1995; :277–293. [PubMed: 8520220]
69. Lee W, Tonelli M, Markley JL. Bioinformatics. 31 2015; :1325–1327. [PubMed: 25505092]

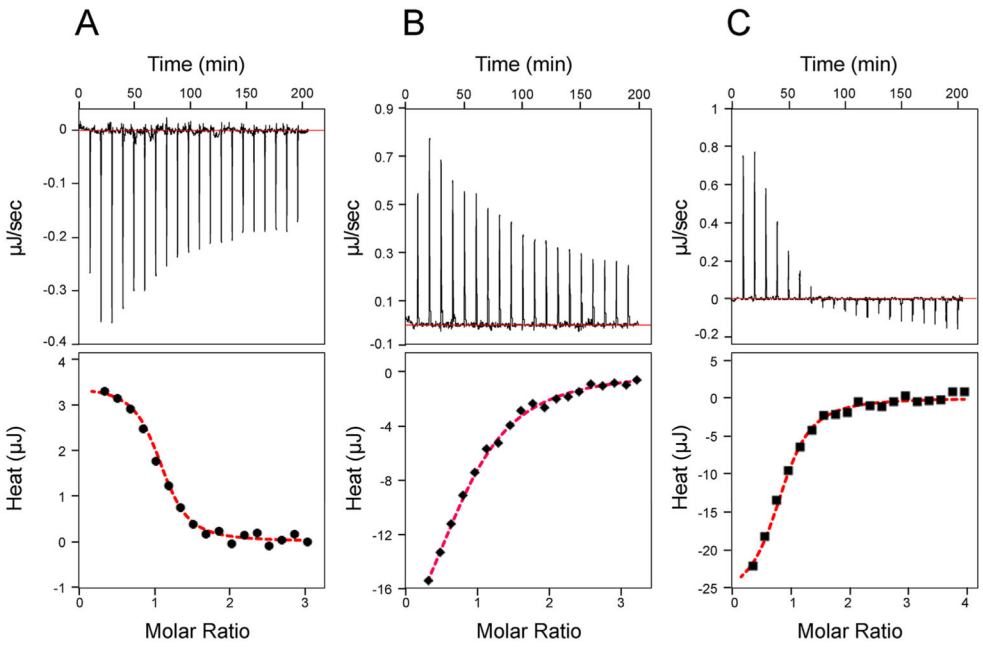

Fig. 1.

ITC analysis of the interactions between $(NIA)_2$ and ISCU, $(NIA)_2$ and FXN, and $(NIAU)_2$ and FXN. Upper panels: peaks indicating heat released after each injection; lower panels: data points fitted to a single 1:1 binding constant to yield thermodynamic parameters. (A) $(NIA)_2$ injected into a solution of ISCU (K_d = 1.7 ± 0.4 µM). (B) $(NIA)_2$ injected into a solution of FXN (K_d = 26.2 ± 2.4 µM). (C) $(NIAU)_2$ injected into a solution of FXN (K_d = 3.0 ± 0.6 µM).

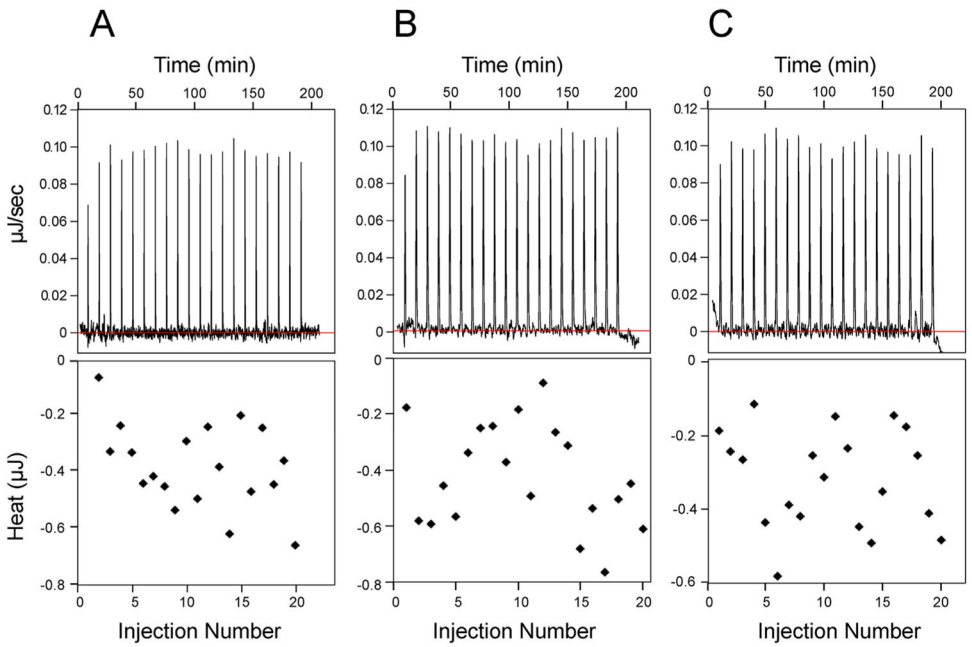

Fig. 2.

Heat of dilution control experiments. (A) 1.1 mM $(NIA)_2$ was injected into HNT buffer. (B) HNT buffer was injected into 0.1 mM ISCU. (C) HNT buffer was injected into 0.1 mM FXN. Upper panels: peaks indicating heat released after each injection; lower panels: total heat generated from each injection. The resulting heat of dilution is negligible in all cases.

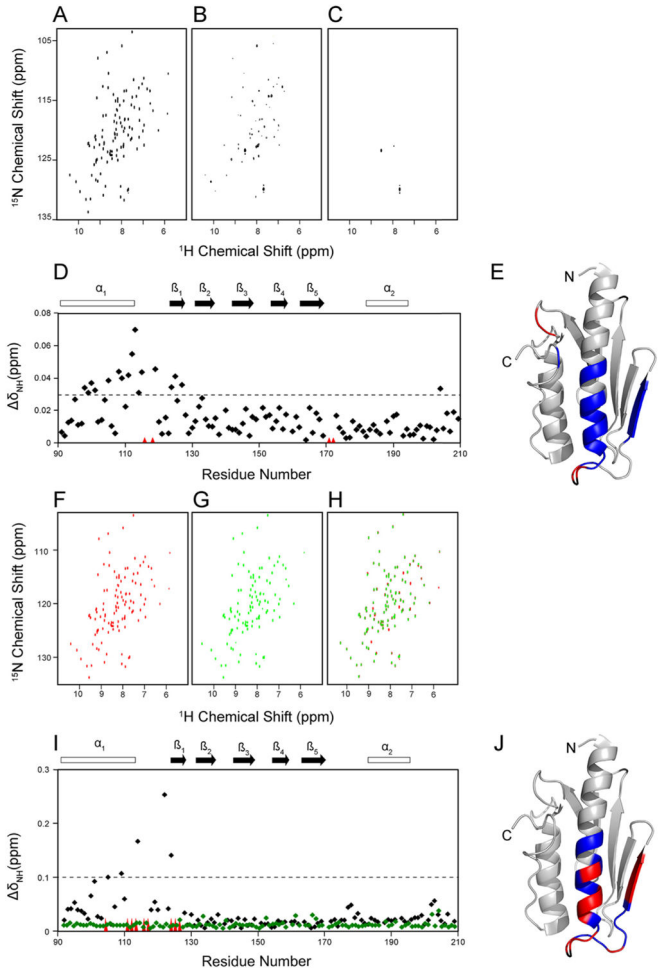

Fig. 3.

NMR evidence showing that $(NIA)_2$ and Fe^{2+} share the same binding site on FXN. (A) 2D $^{1}H,^{15}N$ TROSY-HSQC spectrum of [U-^{15}N]-FXN. (B) 2D $^{1}H,^{15}N$ TROSY-HSQC spectrum of [U-^{15}N]-FXN following the addition of 1.0 subunit equivalent of unlabeled $(NIA)_2$. (C) 2D $^{1}H,^{15}N$ TROSY-HSQC spectrum of [U-^{15}N]-FXN following the addition of 1.0 subunit equivalent of unlabeled $(NIA)_2$ and 1.0 equivalent ISCU. (D) CS perturbation ($\Delta\delta_{NH}$) of the $^{1}H,^{15}N$ signals of [U-^{15}N]-FXN resulting from its interaction with $(NIA)_2$. Red triangles denote residues whose signals were broadened beyond detection; perturbations above the dashed line are considered to be significant. (E) CS perturbation result of panel D mapped onto the structure of FXN (Protein Data Bank (PDB): 1ekg) [47]. Color code: green, not significantly affected ($\Delta\delta_{NH}$ < 0.03 ppm); blue, significant chemical shift changes ($\Delta\delta_{NH}$ > 0.03 ppm); red, severe line broadening; black, no assignments. (F) $^{1}H,^{15}N$ TROSY-HSQC spectrum of [U-^{15}N]-FXN. (G) $^{1}H,^{15}N$ TROSY-HSQC spectrum of [U-^{15}N]-FXN after the addition of 2.0 equivalent of Fe^{2+}. (H) Overlay of the spectra from panels F and G. (I) CS perturbation ($\Delta\delta_{NH}$) of the $^{1}H,^{15}N$ signals of [U-^{15}N]-FXN resulting from binding Fe^{2+} (black) and Fe^{3+} (green). The red triangles denote the residues whose signals disappeared after binding Fe^{2+}; perturbations above the dashed line are considered to be significant. (J)

CS perturbation result of panel F mapped onto the structure of FXN (PDB: 1ekg). Color code as in E.

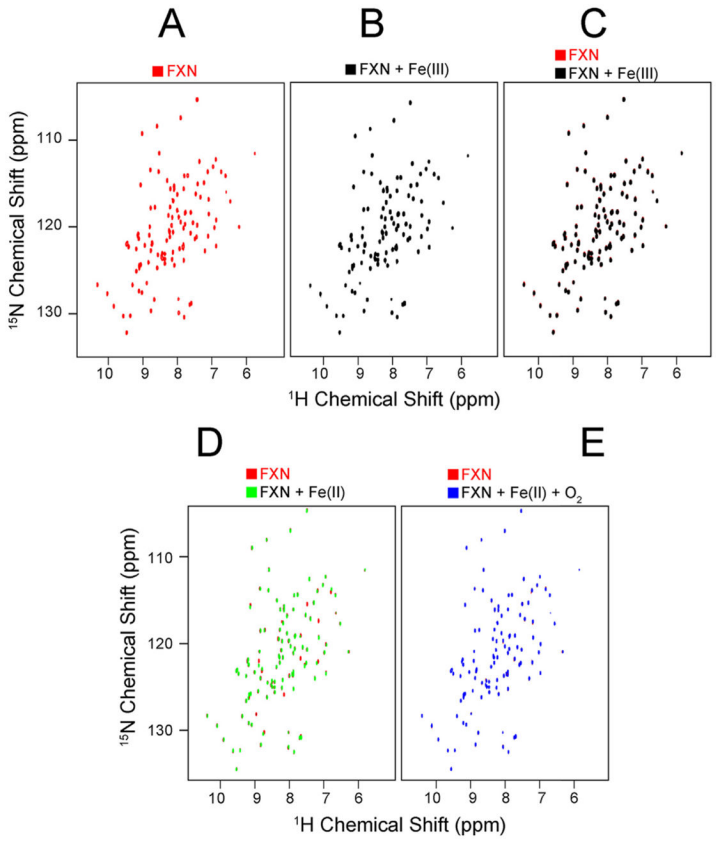

Fig. 4.

NMR evidence showing that FXN does not bind Fe^{3+}. (A) $^{1}H,^{15}N$ TROSY-HSQC spectrum of [U-^{15}N]-FXN. (B) $^{1}H,^{15}N$ TROSY-HSQC spectrum of [U-^{15}N]-FXN after the addition of a 5-fold molar excess of Fe^{3+}. (C) Overlay of the spectra from panels A and B, showing no difference between the two spectra. (D) Overlay of the $^{1}H,^{15}N$ TROSY-HSQC spectra of FXN alone (red) and FXN + Fe(II) (green); note that bound Fe(II) leads to disappearance of many FXN signals as the result of paramagnetic line broadening. (E) Overlay of spectra of FXN alone (red) and FXN + Fe(II) following air oxidation. Conversion of Fe(II) to Fe(III) led to its release from the protein as indicated by the absence of chemical shift perturbations.

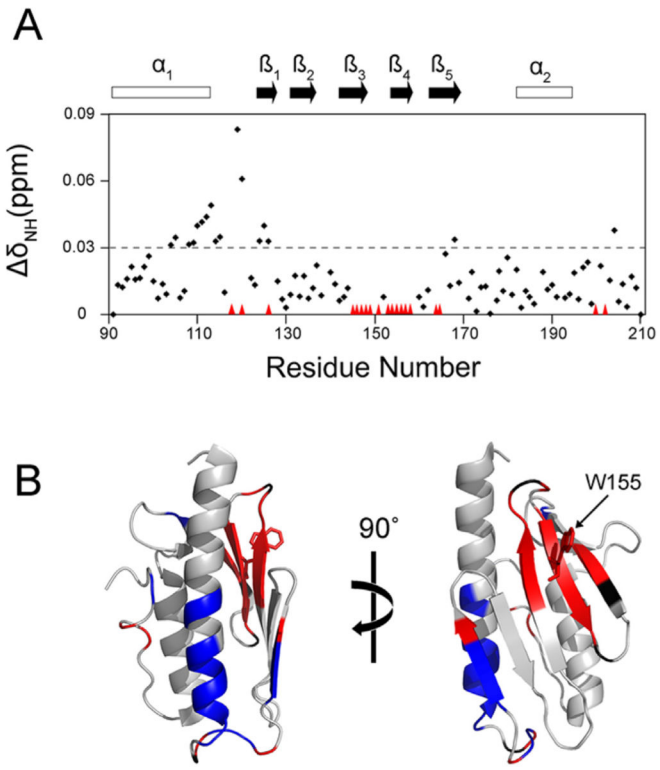

Fig. 5.

NMR evidence concerning the interaction between FXN and $(NIAU)_2$. (A) CS perturbation ($\Delta\delta_{NH}$) of the $^{1}H,^{15}N$ signals of [U-^{15}N]-FXN resulting from its interaction with $(NIAU)_2$; perturbations above the dashed line are considered to be significant. (B) CS perturbation results from panel C mapped onto the structure of FXN (PDB: 1ekg). Color code: green, not significantly affected ($\Delta\delta_{NH} < 0.03$ ppm); blue, significant chemical shift changes ($\Delta\delta_{NH} > 0.03$ ppm); red, severe line broadening; black, no assignments.

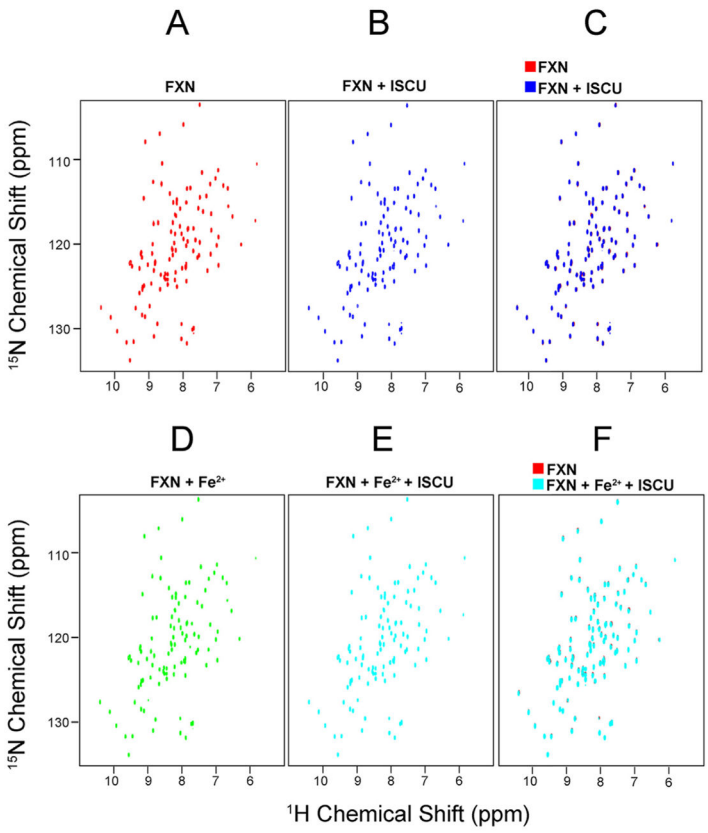

Fig. 6.

NMR evidence showing that FXN (without or with bound Fe^{2+}) does not interact with ISCU in the absence of $(NIA)_2$. (A) $^{1}H,^{15}N$ TROSY-HSQC spectrum of [U-^{15}N]-FXN. (B) $^{1}H,^{15}N$ TROSY-HSQC spectrum of sample from A following the addition of 1.0 equivalent of unlabeled ISCU. (C) Overlay of the spectra from panels A and B. (D) $^{1}H,^{15}N$ TROSY-HSQC spectrum of [U-^{15}N]-FXN after the addition of 2.0 equivalent of Fe^{2+}. (E) $^{1}H,^{15}N$ TROSY-HSQC spectrum of sample from D following the addition of 2.0 equivalents of unlabeled ISCU. (F) Overlay of the spectra from panels E and A. The $^{1}H,^{15}N$ TROSY-HSQC spectrum of [U-^{15}N]-Fe^{2+}-FXN + ISCU is the same with that of [U-^{15}N]-FXN, indicating iron transfer from FXN to ISCU and no interaction between ISCU and FXN after iron transfer.

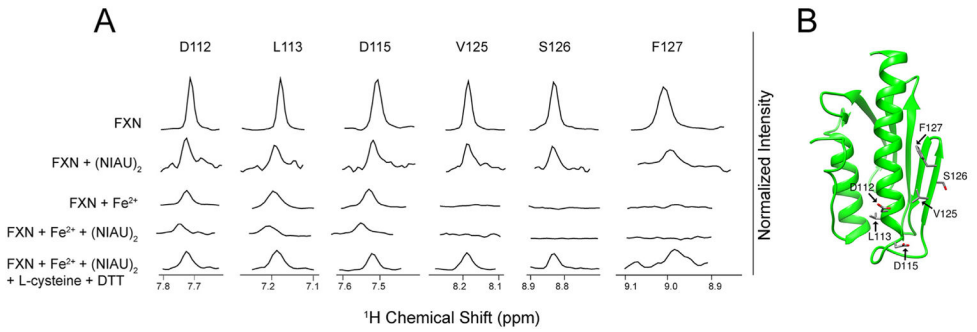

Fig. 7.

Results showing that Fe^{2+} bound to FXN remains bound when FXN interacts with $(NIA)_2$ but becomes labile upon the addition of L-cysteine and DTT. (A) One-dimensional sections along the ^{1}H-dimension from two-dimensional $^{1}H,^{15}N$ TROSY-HSQC peaks assigned to residues D112, L113, D115, V125, S126 and F127 under conditions specified in the figure. (B) Structure of FXN (PDB: 1ekg) indicating the positions of the residues studied.

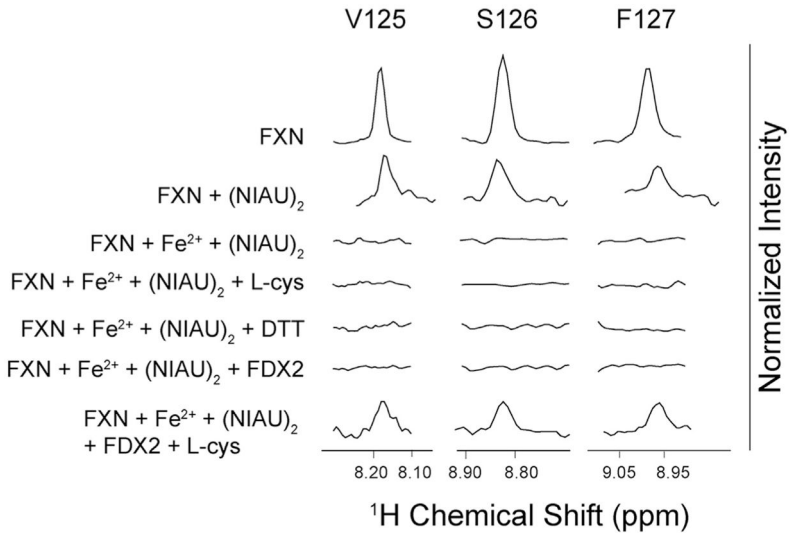

Fig. 8.

One-dimensional ^{1}H chemical shift slices from two-dimensional $^{1}H,^{15}N$ TROSY-HSQC spectra of [U-^{15}N]-FXN at the positions of residues V125, S126, and F127 under the conditions specified in the figure.

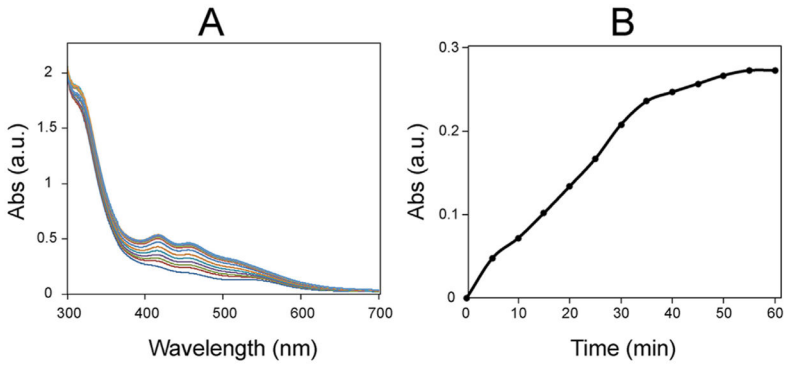

Fig. 9.

Fe-S cluster assembly reaction using Fe^{2+}-FXN as the iron source and reduced FDX2 as the electron donor. The Fe-S cluster reconstitution mixture contained 5 μM $(NIA)_2$, 50 μM ISCU, 100 μM Fe^{2+}-FXN, 100 μM reduced FDX2. The reaction was initiated by the addition of 250 μM L-cysteine (A) uv/vis spectra taken every 5 min for 60 min after initiation of the reaction (B) Increase of absorbance at 456 nm (normalized) as an indication of Fe-S cluster assembly. Previous studies from this laboratory have shown that the absorbance at 456 nm reflects cluster assembly and not simply the oxidation of ferredoxin [14].